

# Scanning optical homodyne detection of high-frequency picoscale resonances in cantilever and tuning fork sensors

G. Zeltzer and J. C. Randel

*Department of Applied Physics, Stanford University, Stanford, California 94305, USA*

A. K. Gupta<sup>a)</sup> and R. Bashir

*Birck Nanotechnology Center, School of Electrical and Computer Engineering, Purdue University, West Lafayette, Indiana 47907, USA*

S.-H. Song<sup>b)</sup> and H. C. Manoharan<sup>c)</sup>

*Department of Physics, Stanford University, Stanford, California 94305, USA*

(Received 1 September 2007; accepted 9 October 2007; published online 26 October 2007)

Higher harmonic modes in nanoscale silicon cantilevers and microscale quartz tuning forks are detected and characterized using a custom scanning optical homodyne interferometer. Capable of both mass and force sensing, these resonators exhibit high-frequency harmonic motion content with picometer-scale amplitudes detected in a 2.5 MHz bandwidth, driven by ambient thermal radiation. Quartz tuning forks additionally display both in-plane and out-of-plane harmonics. The first six electronically detected resonances are matched to optically detected and mapped fork eigenmodes. Mass sensing experiments utilizing higher tuning fork modes indicate greater than six times sensitivity enhancement over fundamental mode operation. © 2007 American Institute of Physics. [DOI: 10.1063/1.2803774]

Since its invention in 1986 the atomic force microscope (AFM) has relied on the deflection of a spring-mass system, originally engineered as a cantilever terminated with a sharp tip,<sup>1</sup> responding to very small external forces exerted between the tip and probed surface. The introduction in 1991 of the frequency-modulated AFM scheme allowed enhanced force sensitivity without a trade-off in operating speed.<sup>2</sup> Gains in measurement speeds were achieved by increasing the fundamental resonant frequency  $\omega_0 = \sqrt{k_{\text{eff}}/m}$  from the initial  $\sim 10^2$  to  $\sim 10^5$  Hz. The sensor spring constants in use have increased from the originally soft  $\sim 0.01$  N/m for silicon micromachined cantilevers to much stiffer  $\sim 3000$  N/m quartz tuning fork devices. The latter proved to be a higher-speed and high- $Q$  alternative, possessing intrinsic piezoelectric properties characteristic to quartz crystals.<sup>3</sup> The piezoelectric response of the fork, linking the mechanical motion to an electric signal, greatly simplifies AFM design by allowing a compact and simple readout. The tuning fork performance is remarkable both at room temperature and in cryogenic environments.<sup>4</sup> In most cases the mechanical excited motion of the fork is the fundamental symmetric in-plane mode.<sup>5</sup> In contrast to the fundamental mode, higher harmonics are predicted to carry information on the interaction between tip and sample.<sup>6</sup> Electronically detected higher harmonics have led to subatomic AFM features<sup>7</sup> and increased measurement speed.<sup>8</sup> Recently, the use of higher harmonic detection in cantilever type sensors demonstrated the capability to measure local sample stiffness<sup>9</sup> and the contact potential of  $C_{60}$  adsorbed on graphite.<sup>10</sup> Mass detection in cantilever based measurements was shown to benefit from enhanced sensitivity at higher modes.<sup>11</sup> Thus, quantitative

knowledge of the higher harmonic content of cantilever and tuning fork sensors directly feeds into the design of next-generation nanoprobbers.

In this letter, we present picoscale characterization based on a scanning homodyne interferometric scheme allowing detection of high-frequency oscillation modes in micromachined devices. Interferometric detection of cantilever motion has been shown to possess sub-nanometer sensitivity in static and low-frequency AFM cantilever deflection<sup>12-14</sup> as well as in higher bandwidth mass sensing applications.<sup>15</sup> Here, a free space Michelson interferometer [Fig. 1(a)], with micrometer-scale spot size in the active arm, enables picometer-scale oscillatory motion detection up to 200 MHz. A coherent and polarized Gaussian beam originating from a 20 mW HeNe laser ( $\lambda=632.8$  nm) is expanded and collimated by means of an expansion module delivering a beam waist  $w_{\text{beam}}=3$  mm. The beam is split using a polarizing beam splitter and focused in the active arm of the interferometer by a  $10\times$  microscope objective ( $f=15$  mm) to spot size  $w_{\text{spot}}=4\lambda f/3\pi w_{\text{beam}}=1.3$   $\mu\text{m}$ . A custom built low-noise and high-speed transimpedance amplifier, with a gain of  $10^7$  V/A, amplifies the photocurrent of a reverse-biased high-speed silicon p-i-n photodiode allowing low intensity fringe detection in a 200 MHz bandwidth. The optomechanical setup is simple and robust to vibrations when built on a dedicated optical breadboard, offering a relatively inexpensive solution and measurement accuracy comparable to commercially available laser Doppler vibrometers. We apply this technique to sensors of different designs and materials, but matching resonant frequencies.

A benchmark of the measurement capability of such a system is given in Fig. 1(c). Thermally excited modes in a bandwidth of 1.5 MHz of a silicon cantilever [Fig. 1(b)], with length  $l=90$   $\mu\text{m}$ , width  $w=8$   $\mu\text{m}$ , and thickness  $t=200$  nm, are detected as peaks in the amplitude spectral density (ASD) of oscillation when the interferometer is po-

<sup>a)</sup>Present address: BioMEMS Resource Center, Massachusetts General Hospital, Harvard Medical School, Boston, Massachusetts 02114, USA.

<sup>b)</sup>Permanent address: School of Electrical and Electronics Engineering, Chung-Ang University, Seoul 156-756, Korea.

<sup>c)</sup>Electronic mail: manoharan@stanford.edu

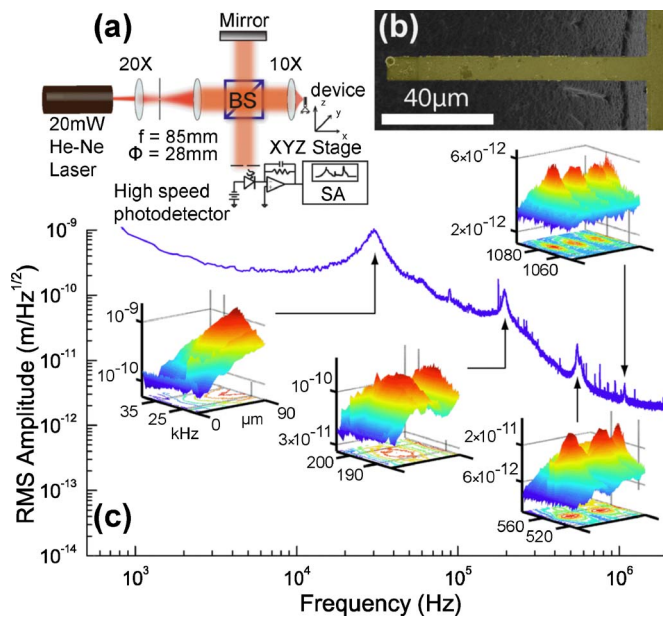


FIG. 1. (Color online) (a) Scanning Michelson interferometer including a beam expander (focal length  $f$  and diameter  $\phi$ ) and focusing lens. (b) Scanning electron microscope image of 200-nm-thick Si cantilever. (c) High frequency cantilever free-end motion ASD. (Insets) Cantilever maps of ASD vs position for the first four flexural modes.

sitioned at the cantilever free end. Thermal motion in such devices was previously used to detect femtogram virus particles binding on the cantilever beam surface.<sup>16</sup> Using the analytically computed eigenfrequencies of the cantilever beam,<sup>17</sup>  $f_n = (\alpha_n^2/2\pi) \sqrt{Et^2/12\rho l^4}$  with  $\alpha_{1,\dots,4} = 1.875, 4.694, 7.855, \text{ and } 10.996$ ,  $\alpha_{5,\dots,n} = \pi(n-1/2)$ , mass density  $\rho$ , and elastic modulus  $E_{\text{Si}(110)} = 169$  GPa, the first four flexural mode frequencies compute to  $f_n = 34.0, 212.8, 596.0, \text{ and } 1167.9$  kHz. These values agree well with measured frequencies of 30.6, 194.1, 549.1, and 1080.2 kHz. Scanning and recording the ASD at  $1 \mu\text{m}$  increments along the cantilever enables mapping of the eigenmodes presented in the insets of Fig. 1(c). An interesting fact observed in the higher modes is the apparent increase in the  $Q$  of each mode from 20 for the fundamental at 31 kHz to 50 at 1.08 MHz. Braun *et al.*<sup>11</sup> have shown that the distributed mass sensitivity of a liquid-submerged cantilever increases with the mode frequency. For our sensors, an enhanced mass sensitivity  $S = \delta f / \delta m$  is foreseeable at higher modes for detection of concentrated mass, well beyond  $S = 0.21$  Hz/fg given by fundamental mode operation only. Indeed this sensitivity should further benefit from the fact that the observed  $Q$  of the cantilever does not degrade for higher harmonics.

The tuning fork is an assembly of two cantilevers with intrinsic piezoelectric response and proven high sensitivity in AFM measurements. We optically and electrically characterize a commercial unit with a tine length of  $l = 2450 \mu\text{m}$ , width  $w = 120 \mu\text{m}$ , and thickness  $t = 220 \mu\text{m}$ . The theoretical spring constant is obtained from  $k = Ewt^3/4l^3 = 1709$  N/m, where  $E_{\text{quartz}} = 78.7$  GPa. The tine displacement is measured by the interferometer with the active beam arm reflecting off the surface of one of the tines, as shown in Fig. 2(a).

Positioning the interferometer at the free end of one of the fork tines and driving the fork at resonance with variable excitation voltages allows the calibration of the fork amplitude response. In Fig. 2(b) the photodetector signal is re-

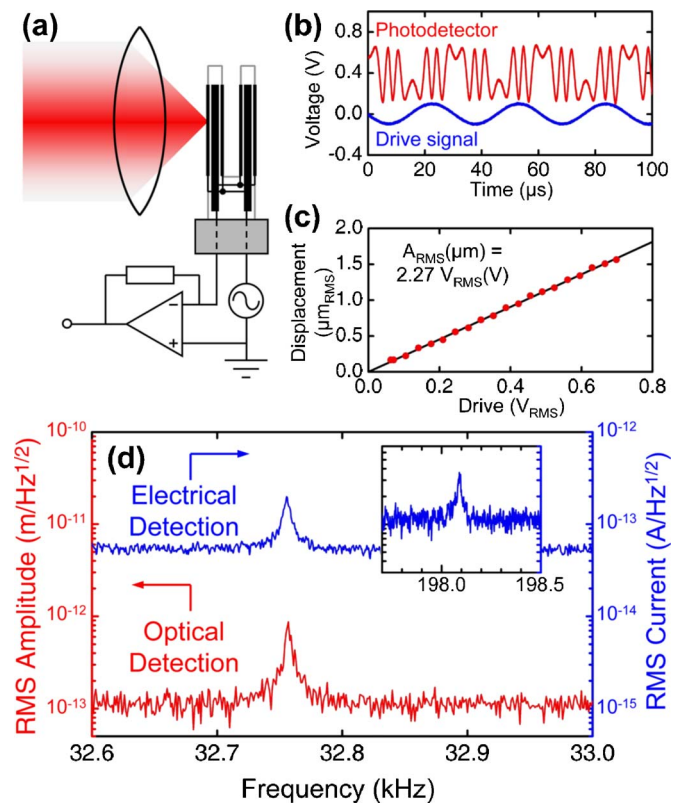


FIG. 2. (Color online) (a) Tuning fork simultaneous optical/electrical measurement setup. (b) Interferometer readout for large fork drive signal. (c) Tuning fork amplitude vs excitation voltage. (d) Room temperature tuning fork thermal motion detected optically at the fundamental and electrically at the fundamental and second harmonic in-plane modes.

corded while the fork is subjected to drive signal  $V(t) = V_0 \cos \omega t$  with  $V_0 = 90$  mV and  $f_0 = \omega/2\pi = 32756$  Hz (the experimentally determined fundamental frequency).

In Fig. 2(c) we plot measured amplitude  $A$  versus  $V_0$  to obtain the displacement sensitivity  $\gamma$  from the slope.  $A$  is related to the piezoelectric strain constant  $d_{21}$  and the surface charge  $q$  on each electrode by  $q/A = 12d_{21}kl_e(l-l_e/2)/t^2$ , where  $l_e$  is the electrode length.<sup>4</sup> Taking a time derivative and replacing the spring constant  $k$  with the theoretical value, we arrive at an expression for the fork sensitivity,

$$\gamma = \left[ 12\pi d_{21} E f_0 Z \left( \frac{wtl_e}{l^3} \right) \left( l - \frac{l_e}{2} \right) \right]^{-1}, \quad (1)$$

where  $Z$  is the magnitude of the fork's complex impedance. Setting  $d_{21} = 2.31 \times 10^{-12}$  C/N,  $Z = 330$  k $\Omega$ , and  $l_e = 1.6$  mm, we find  $\gamma = 2.8 \mu\text{m}/\text{V}$ . This agrees well with the experimentally observed value of  $2.27 \mu\text{m}/\text{V}$ . With the fork electrodes shorted, thermally excited motion is detected optically at the fundamental frequency, as shown in Fig. 2(d). The optically detected integrated amplitude is  $x_{\text{rms}} = 1.58$  pm. This is in excellent agreement with the expected value from equipartition,  $x_{\text{rms}} = \sqrt{k_B T/k} = 1.56$  pm, using  $T = 300$  K and the theoretical  $k$ . Also shown in Fig. 2(d) is the simultaneous piezoelectric current generated by thermally excited motion at the first two harmonics.

We proceed with identifying the higher eigenmodes of the fork, with both in-plane and out-of-plane amplitude components. Figure 3(d) displays the ASD of these detected modes with the readout point at the free end of the fork. Treating the fork as a cantilever, the in-plane resonance fre-

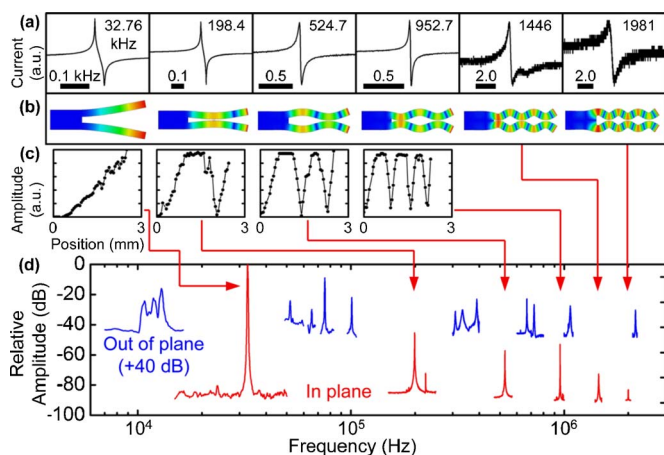


FIG. 3. (Color online) (a) Tuning fork resonances detected via conductance vs drive frequency in a 2 MHz bandwidth. (b) FEA-computed mode shapes for the first six symmetric in-plane eigenmodes. (c) Optically detected mode shapes for the first four in-plane eigenmodes. (d) Fork free-end optically detected in-plane and out-of-plane resonances using swept sine excitation. Amplitudes normalized to the in-plane fundamental mode.

quencies are computed at 32.2, 201.9, 565.3, 1107.7, 1830.9, and 2735.1 kHz, which approximate well only the first three experimental values. However, finite-element analysis (FEA) of the entire device reproduces the experimental results with better than 5% accuracy [see computed mode shapes in Fig. 3(b)]. We are able to scan the entire 2.4 mm tine and map the first four modes at 32.756, 198.1, 528.075, and 958.225 kHz [Fig. 3(c)]. The mode shapes for the resonances at 1453.85 and 2000.42 kHz are inferred as the fifth and sixth symmetric modes. Conductance measurements shown in Fig. 3(a) were carried out with the fork placed in vacuum ( $\leq 0.1$  Torr). The frequencies of these resonances match the first six in-plane optical values indicating that the piezoelectric coupling is maximized at these modes. Electrical excitation of the out-of-plane modes led to very small amplitudes (in the nanometer range for driving voltages up to 10 V). This is equivalent to out-of-plane motion approximately 3 orders of magnitude smaller than in-plane modes [see Fig. 3(d)].

A mass sensing experiment was carried out in vacuum by attaching a 120 ng load to one tine of the fork. The first

four electrically detected modes experienced frequency shifts of 50, 148, 221, and 305 Hz, indicating over sixfold improvement in mass sensitivity  $S$  for operation at the fourth mode over the fundamental mode. Compared to Si, the minimum detectable mass with a quartz tuning fork also benefits from a  $>100$  times boost in  $Q$  ( $>10^5$  in vacuum). An observed  $\sqrt{f_n}$  dependence of the  $n$ th harmonic frequency shift is currently under investigation.

We conclude that higher oscillatory modes can be used to achieve higher speed and sensitivity for both force and mass sensing applications. The experimental mode shape identification can be used in optimizing sensing tip and mass positions within nanoprobe setups.

This work was supported by NSF (Stanford-IBM Center for Probing the Nanoscale and CAREER Program) and ONR (YIP/PECASE). We acknowledge fellowship support from NSF (J.C.R), SBS Foundation (S.-H.S), and the Alfred P. Sloan Foundation (H.C.M). We thank D. Weld and T. Kopley for discussions.

<sup>1</sup>G. Binnig and C. F. Quate, Phys. Rev. Lett. **56**, 930 (1986).

<sup>2</sup>T. R. Albrecht, P. Grütter, D. Horne, and D. Rugar, J. Appl. Phys. **69**, 668 (1991).

<sup>3</sup>F. J. Giessibl, Appl. Phys. Lett. **73**, 3956 (1998).

<sup>4</sup>F. J. Giessibl, Appl. Phys. Lett. **76**, 1470 (2000).

<sup>5</sup>T. D. Rossing, D. A. Russel, and D. E. Brown, Am. J. Phys. **60**, 620 (1992).

<sup>6</sup>U. Dürig, New J. Phys. **2**, 5.1 (2000).

<sup>7</sup>S. Hembacher, F. J. Giessibl, and J. Mannhart, Science **305**, 380 (2004).

<sup>8</sup>S. Liu, J. L. Sun, H. S. Sun, X. J. Tan, S. Shi, J. H. Guo, and J. Zhao, Chin. Phys. Lett. **20**, 1928 (2003).

<sup>9</sup>O. Sahin, C. F. Quate, and O. Solgaard, Phys. Rev. B **69**, 165416 (2004).

<sup>10</sup>S. Sadewasser, G. Villanueva, and J. A. Plaza, Appl. Phys. Lett. **89**, 033106 (2006).

<sup>11</sup>T. Braun, V. Barwich, M. K. Ghatkesar, A. H. Bredekamp, C. Gerber, M. Hegner, and H. P. Lang, Phys. Rev. E **72**, 031907 (2005).

<sup>12</sup>D. Rugar, H. J. Mamin, R. Erlandsson, J. E. Stern, and B. D. Terris, Rev. Sci. Instrum. **59**, 2337 (1988).

<sup>13</sup>C. Schonenberger and S. F. Alvarado, Rev. Sci. Instrum. **60**, 3131 (1989).

<sup>14</sup>R. Erlandsson, G. M. McClelland, C. M. Mate, and S. Chiang, J. Vac. Sci. Technol. A **6**, 266 (1988).

<sup>15</sup>N. V. Lavrik and P. G. Datskos, Appl. Phys. Lett. **82**, 2697 (2003).

<sup>16</sup>A. Gupta, D. Akin, and R. Bashir, Appl. Phys. Lett. **84**, 1976 (2004).

<sup>17</sup>D. Sarid, *Scanning Force Microscopy* (Oxford University Press, New York, 1994), pp. 9–11.